Cassini In-Flight Navigation Adaptations

Duane C. Roth,[1] Yungsun Hahn,[2] William M. Owen Jr.,[3] and Sean Wagner[4]
Jet Propulsion Laboratory, California Institute of Technology, Pasadena, CA, 91109, USA

In the nearly two decades of Cassini flight, adaptations to navigation processes were applied as characteristics unique to Cassini were identified and spacecraft configuration changes were implemented. Additionally, operational experience was leveraged into more efficient processes, better modeling, and more robust contingency strategies. Trajectory adjustments were implemented to allow further investigation of surprising science discoveries meriting more attention. Unique analyses were performed to determine how to best accomplish atypical science observations while maintaining acceptable risk levels. Descriptions of the most significant adaptations are organized according to the affected navigation subsystems: trajectory design, orbit determination, optical navigation, and maneuver design.

I. Introduction

NASA'S Cassini Mission to Saturn was immensely successful. All science goals were attained, with Cassini observations leading to many astounding discoveries such as a methane cycle on Titan analogous to Earth's water cycle, an ocean of salty water below Enceladus' frozen crust suggesting the possibility of alien microbial life, and Enceladus' ice geysers as the source of Saturn's E-ring. The European Space Agency's (ESA) Huygens probe, carried to Saturn aboard the Cassini orbiter and successfully landed on Titan's surface, was the first spacecraft to land on a world in the outer solar system. Its suite of instruments characterized Titan's dense atmosphere during descent and surface properties after surviving a soft landing. Navigation of the Cassini spacecraft played an essential role in enabling these discoveries and achieving all science mission goals. Sub-kilometer target misses were routinely achieved in the final years of the mission, not only satisfying tight science pointing and timing requirements, but also ensuring adequate propellant margins through the end of Cassini's second extended mission. With its propellant tanks nearly depleted, the Cassini spacecraft met a fiery demise September 15, 2017 as it was intentionally guided into Saturn's atmosphere deep enough to become captured, thereby satisfying planetary protection requirements.

Launched October 15, 1997, the first seven years of the mission involved travel from Earth to Saturn. A Titan IVB/Centaur launch system and gravity assists at Venus (twice), Earth, and Jupiter provided the energy required to reach Saturn. Saturn Orbit insertion (SOI) took place July 1, 2004, nineteen days after the first targeted satellite encounter, a 2000 km flyby of Saturn's largest irregular moon Phoebe. The next thirteen years spanned prime mission and two extended missions, the Equinox and Solstice Missions, with 127 targeted encounters of Saturn's largest moon Titan and several more of the smaller icy satellites. A listing of all targeted encounters, along with selected information about the orbit resulting after each encounter, is provided for each mission in the Appendix. Nomenclature for a targeted encounter starts with the first letter of the satellite encountered, followed by a number. However, the first three Titan targeted flybys were designated with a letter instead of a number. Titan numbering began at T3, after Ta, Tb, and Tc.

With the mission now over, a description of several operational adaptations and key mission aspects are provided from launch to Saturn atmospheric entry. Future planetary system tour missions in the planning stages may draw upon this material to gain an understanding of the challenges and expectations ahead of them.

II. Trajectory Design Adaptations

Navigators implemented global reference trajectory updates to re-optimize trajectories, reducing ΔV costs as satellite ephemerides changed and accuracies improved via the filtering of orbital tracking data and optical navigation

---

[1] Delivery Manager, Mission Design and Navigation Section.
[2] Navigation Engineer, Mission Design and Navigation Section.
[3] Principal Member of Technical Staff, Mission Design and Navigation Section.
[4] Navigation Engineer, Mission Design and Navigation Section, AIAA member.

images. Global updates were generally small-scale changes affecting the entire mission. As satellite ephemeris knowledge converged and environmental risk factors became better understood, global updates became less frequent and became absorbed in local updates. Local updates were large scale changes affecting only a small portion of the mission and were implemented to enable new observations (often in response to mission discoveries), improve existing observations, or reduce mission risk. The introduction of a new reference trajectory into flight operations was carefully synchronized with the development of command sequences to avoid re-work of observations that had already progressed through the detailed sequence development process. Table 1 lists the reference trajectory update identifier, dates each became operational, command sequences and trajectory events they spanned, and main motivation for each update [1]. Command sequences typically spanned 5 week intervals during Prime and Equinox Missions and 10 week intervals in Solstice Mission.

Table 1. Reference Trajectory Updates and Motivation.

Reference Trajectory	Operational Start Date	Command Sequence Span	Trajectory Event Span	Main Motivation for Update
030201	Pre-Tour	S01 – S02	SOI – pre-Ta	Initial tour reference trajectory
040513	Jul 30, 2004	S03	SOI – pre-Ta	Re-optimization based on latest ephemeris
040622	Sep 12, 2004	S04	SOI – pre-Ta	Constrain 040513 downstream trajectory shifts
041001	Oct 18, 2004	S05 – S07	Ta – Tc	Raise rev C Iapetus altitude
041210	Jan 22, 2005	S08 – S11	T3 – T5	Raise T5, T7 altitudes to reduce tumble risk
050505	Jun 18, 2005	S12	E2 – pre-T6	Lower Tethys, E2, and H1 altitudes
050720	Jul 31, 2005	S13 – S19	T6 – T12	Raise T7 altitude to reduce tumble risk
060323	Apr 22, 2006	S20 – S29	T13 – T29	Raise Titan flybys, lower E3, add rev 28 occ.
070209	May 4, 2007	S30 – S35	T30 – T38	Resolve I1 imaging/occultation science conflict
070918	Dec 15, 2007	S36 – S41	T39 – T44	Add Equinox Mission, raise E3
080520	Jul 1, 2008	S42 – S45	T45 – T47	Fine tune E5, move 3 maneuvers
080806	Nov 26, 2008	S46 – S56	T48 – T65	Add leap second to auxiliary (OPTG) file
090721	Jan 23, 2010	S57 – S59	T66 – E9	Add Solstice Mission, lower E10 occultation
091005	May 17, 2010	S60 – S71	E10 – T80	Move 5 maneuvers
110818	Jan 24, 2012	S72 – S86	T81 – T107	Move 1 maneuver, re-optimization
140114	Dec 17, 2014	S87 – S93	T108 – T118	Add rev 233 Enceladus plume occultation
150901	Apr 18, 2016	S94 – S101	T119 – EOM	Add Saturn atmosphere model

The initial prime and extended mission reference trajectories provided to the project for tour planning purposes were 030201 for Prime Mission, 070918 for Extended Mission, and 090721 for Solstice Mission. The 030201 trajectory was updated with 040513 for sequence S03, starting only 29 days after Saturn Orbit Insertion. Approach optical navigation images (opnavs) tremendously improved the accuracy of Saturn's satellite ephemerides, quickly rendering 030201 obsolete. When 040513 was released, navigators had not yet realized that adding a few minor constraints to the trajectory optimization process could greatly reduce downstream event time shifts and the related re-sequencing workload. The next update, 040622, utilized these constraints to mitigate the "ripples" introduced in 040513.

Four updates in Table 1 raised flyby altitudes to reduce risk to the spacecraft's health and prevent loss of science data. In 041210, 050720, and 060323, navigators raised Titan altitudes to prevent spacecraft tumbling due to a denser-than-expected atmosphere. Extrapolating density estimates from previous Titan flybys, it appeared that Cassini may not have had sufficient control authority to maintain attitude during the lower altitude flybys. Tumbling would have resulted in loss of attitude knowledge, entry to safe mode, and loss of high value flyby science data. The 060323 update benefited from an improved Titan atmosphere model based on results from several previous Titan flybys. The new model was combined with each planned spacecraft flyby attitude to predict torques on the spacecraft and determine the lowest flyby altitude that would maintain acceptably low spacecraft tumbling probabilities. Nearly all of the low Titan flybys required an increased altitude. The fourth update to raise an altitude was 070918. The E3 altitude was raised from 25 km to 50 km to reduce possible hazards from debris in the newly discovered Enceladus plume.

A few updates enabled new or, in the case of the Huygens probe mission, re-enabled existing key science observations. Cassini's trajectory during the Huygens probe mission was redesigned to mitigate a design flaw discovered in the Huygens receiver. The only targeted quality Tethys flyby was enabled with 050505 and a unique Enceladus plume occultation was enabled with 141014. The Tethys flyby is described in [2]. The other topics are discussed more fully in the next two subsections. The remaining trajectory updates mostly served to improve existing science observations. The 070209 update resolved a conflict between a stellar occultation and high resolution imaging of Iapetus at closest approach during the only targeted flyby of the satellite [3]. The update moved the stellar occultation away from periapsis and altered the Iapetus ground track to improve imaging of the satellite's equatorial ridge. Maneuver locations were changed in some updates to remove conflicts with science observations desired at similar times.

Updates 080520 and 080806 are identical. The objective in producing the latter file was to quickly generate an Orbit Propagation & Timing Geometry (OPTG) ancillary file using an automated procedure. The ancillary file included a newly introduced leap second needed for sequence development. Later leap seconds were included in OPTG files without updating the reference trajectory.

A. Huygens Probe Redesign

ESA's Huygens probe mission was originally designed for landing and relay during the first orbit about Saturn and at the first targeted Titan flyby. However, an end-to-end in-flight test of the probe relay link in February 2000 revealed unexpected behavior of the Huygens receiver onboard the Cassini orbiter. The anomaly was traced to a design flaw of the receiver's bit synchronizer, which had a bandwidth too small to accommodate the Doppler shift of the relay signal [4]. Shortly thereafter, a joint ESA/NASA task force, the Huygens Recovery Task Force (HRTF), was established with a mandate to better understand the anomaly and to develop a plan to recover the Huygens mission.

Navigators contributed to the recovery by changing Cassini's trajectory to reduce Doppler shift between the orbiter and probe during the data relay period. The 030201 update reduced the Doppler shift by raising the altitude of the orbiter for the probe delivery encounter from 1200 to 60,000 km so that the radial component of the orbiter's velocity relative to the probe was much smaller. To protect downstream science, navigators isolated these changes to the section of the tour previously dedicated to the probe mission. This required the insertion of an additional orbit and targeted flyby into the tour because a distant flyby at T1 or T2 would not provide sufficient bending to change Cassini's orbit period and re-encounter Titan by T3. By reducing the period of the initial orbit and making the first Titan encounter earlier, the additional orbit and targeted encounter achieved the necessary orbit period to tie back into the original reference trajectory at T3. Orbits T1 and T2 were then replaced by Ta, Tb, and Tc so downstream Titan encounter designations would not need to be incremented. The changes can be seen in Figure 1.

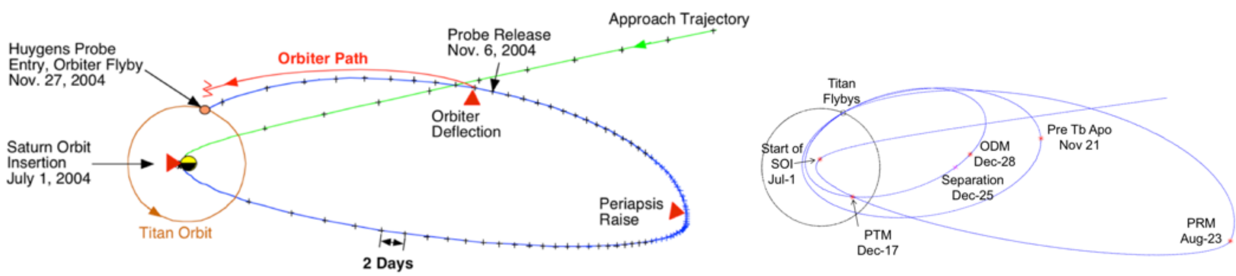

Fig. 1 Huygens Original Trajectory (left) and Redesigned Trajectory (right).

The initial redesign included a 64,000 km altitude non-targeted flyby of Iapetus seven days after probe separation. At first, this flyby was considered a fortuitous bonus, especially since closest approach was on the opposite hemisphere from the only targeted future Iapetus flyby. Upon completion of an orbit determination covariance analysis, however, navigators discovered that the perturbation to Huygens' trajectory due to the uncertainty in Iapetus' gravitational force could prevent the probe flight path angle requirement from being met [5]. The final design, 041001, raised Iapetus' closest approach altitude to 127,000 km by lowering the Tb flyby altitude from 2200 km to 1200 km. This change significantly increased the available margin for error in the Iapetus mass estimate.

Huygens tour redesign used 87 of the 202 m/s ΔV margin available (at the 95% level) from the previously baselined Prime Mission. Of the extra ΔV spent, 75 m/s was spent on larger SOI and Periapsis Raise (PRM) maneuvers to reduce the initial orbit period and move the first Titan flyby 32 days earlier. SOI increases were mitigated by starting the maneuver 9 minutes later, which placed more of the finite burn near periapsis to increase its efficiency. The Probe Targeting Maneuver (PTM) increased by nearly an order of magnitude, from 1.4 to 12.5 m/s, mostly because the period of the probe-delivery orbit had changed from 150 days to 32 days. The increased magnitude also necessitated the addition of a PTM clean-up maneuver. By choosing a retrograde instead of direct distant flyby, the Orbit Deflection Maneuver (ODM) cost was *reduced* from 49 to 26 m/s. Had a direct flyby been maintained, as in the original design, ODM would have cost over 100 m/s [6]. Although the redesigned mission increased ΔV costs, delivery statistics were improved as the first two Titan encounters enabled a better estimate of Titan's ephemeris prior to probe release.

B. Enceladus Plume Occultation

The 140114 update enabled a March 11, 2016 stellar occultation by Enceladus' plume. This high-priority science investigation complemented previous Enceladus plume occultation observations because it was the first and only to be observed near Enceladus' apoapsis: the five previous observations all occurred when Enceladus was closer to periapsis. The latest observation would help scientists determine if water vapor flow was modulated diurnally, similar to ice particles [7]. The ΔV cost of adding this observation was less than 1 m/s and accepted by the Cassini project, even though this observation was near the end of mission and propellant margins were small. Figure 2 shows how Cassini's trajectory was changed as viewed from ε Orionis, the occulted star. Significant trajectory changes to enable this observation began at T115, three targeted flybys before the occultation. Trajectory changes continued to the last targeted flyby, T126, but for the additional reason of setting up the correct asymptote to link to the Grand Finale, the final 22 short-period orbits before Saturn atmospheric entry.

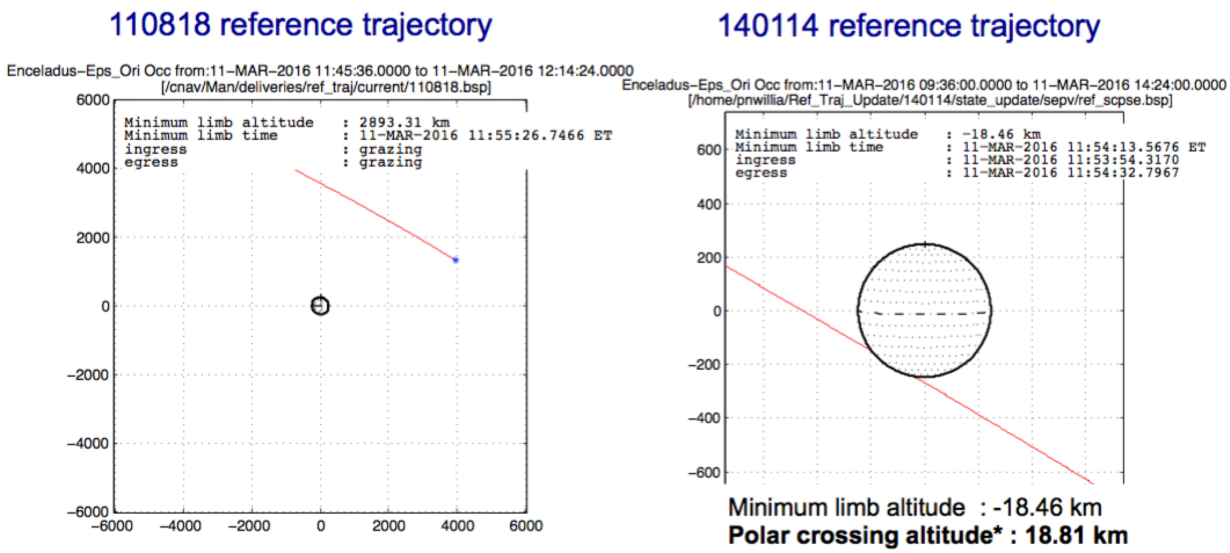

Fig. 2 Enceladus Plume Occultation as Viewed from Epsilon Orion, Before and After Reference Trajectory Update.

III. Orbit Determination Adaptations

Many of the changes implemented in the orbit determination realm were in response to changes in the spacecraft's operational environment and processes. During inner cruise, when the spacecraft was close to the sun, the spacecraft's high gain antenna (HGA) was used as a solar shade and excursions from a HGA-to-sun pointed attitude were small and infrequent. Attitude control was maintained with thrusters. Emphasis was focused on creating adequate non-gravitational force models for solar pressure and asymmetric thermal radiation (induced by the spacecraft's power source). Direct and indirect solar and thermal forces were imparted to the spacecraft, with indirect forces imparted by thruster firings that countered torques from the direct forces. Predictions for ΔVs resulting from engineering maintenance activities were not available, nor were accurate reconstructions from telemetry. In short, there were many nongravitational forces acting on the spacecraft during inner cruise and, with only two tracking passes scheduled per week on average, it was difficult to accurately resolve them. This was not a cause for concern, however, because trajectory accuracy requirements were generally not as demanding as they were later during Saturn orbital operations.

During outer cruise and orbital operations, nongravitational forces were more accurately resolved. Solar pressure and thermal-radiation–induced indirect forces disappeared as attitude control defaulted to reaction wheels instead of thrusters. Solar pressure forces were reduced by two orders of magnitude as the distance from the Sun increased. Thermal radiation forces were exceptionally well determined during three Gravity Wave Experiments conducted near solar oppositions between the Jupiter flyby and Saturn approach. In each of these experiments, the spacecraft remained quiescent and Earth-pointed for several weeks while tracking data was collected continuously. The resulting thermal radiation force estimate was the basis for future thermal force modeling through the end of orbital operations.

Modeling of thruster firings also improved. Thruster activity became more discretized in reaction wheel attitude control mode, with thruster firings for momentum management needed every few days. In thruster attitude control mode, thruster firings for deadband limiting occurred every couple of hours.

A. Iapetus Mass Determination for Huygens Probe Mission

In addition to the Huygens mission trajectory redesign discussed previously, the probe mission also benefited from orbit determination adaptations. Recall the close flyby of Iapetus after probe release and how the uncertainty in Iapetus' gravitational force had put Huygens' entry angle requirement at risk. Mitigating this risk involved not only raising the Iapetus altitude but also better determining the satellite's mass. A mass estimate with error smaller than 7.2 km^3/s^2 was needed at this new altitude to meet entry angle requirements, and estimates were varying by as much as 16 km^3/s^2 [8]. A considerable amount of effort was expended to improve this estimate prior to probe release. A 1.1 million km distant flyby of the satellite that occurred on October 17, 2004 was identified as an opportunity to directly improve Iapetus' mass estimate. During the flyby, the spacecraft was kept in a quiet mode, with no thrusting or turns. Interferometric measurements using the National Radio Astronomy Observatory's Very Long Baseline Array and additional radiometric tracking passes were scheduled to accurately determine the perturbation to Cassini's orbit due to Iapetus before and after the flyby. Iapetus' mass estimate was further improved after the first two Titan flybys improved the ephemeris of Saturn's barycenter, also indirectly improving Iapetus' ephemeris. Ultimately, the value determined prior to probe release (120.55 ± 0.79 km^3/s^2) was found to be consistent with the current reconstructed value (120.5038 ± 0.0080 km^3/s^2 [9]).

More specific orbit determination adaptations include the use of telemetered ΔV information in filtering processes and annual degradation tests of the Y-facing thrusters. These topics are worthy of a more detailed discussion and are presented in the next two subsections.

B. Use of ΔV Telemetry

After successful completion of the Huygens probe mission and at the urging of the navigation team, Cassini spacecraft operators agreed to increase the resolution of telemetered, time-tagged, onboard ΔV computations from spacecraft thrust events. Resolution was increased from 2 to 0.04 mm/s and navigators began including this information in the implementation of dynamical models and in the initialization of filter parameters used in the estimation process.

The primary benefit of telemetry to navigation was rapid convergence of orbit determination after maneuver executions and improved modeling of satellite flybys conducted in thruster mode. Before reaping these benefits, however, its accuracy had to be established. Accuracy estimates were obtained by comparing telemetry computations to navigation team reconstructions of ΔV activity. Reference [10] describes the calibration and evaluation process and provides early orbital mission estimates of the accuracy of maneuver pointing angles derived from the telemetry. Maneuver pointing accuracies were provided for each of the two Cassini propulsive systems, a Main Engine (ME) system for maneuvers larger than 250 mm/s and a Reaction Control System (RCS) for smaller maneuvers. This evaluation was completed near the end of Prime Mission, when 56 ME samples and 35 RCS were available. By end of orbital operations, the number of ME samples had nearly tripled, to 152 samples, and the number of RCS samples had nearly quintupled, to 169 samples. Figures 3 and 4 show differences between navigation reconstructions and telemetry derived computations of maneuver pointing with one-sigma uncertainty bars composed of the RSS of uncertainties from reconstructions and telemetry. Outliers are currently under investigation. Red lines show the mean error. Cumulative distribution functions (CDFs) resulting from all ME samples and all RCS samples are provided in Figure 5. Figures 3–5 are updates of the tables in Reference [10].

After processing maneuver samples through end of mission, estimates of ME accuracies had barely changed. One-sigma normalized Right Ascension uncertainties (normalized RA uncertainty is angle subtended by RA uncertainty in plane defined by zero declination) had changed from 0.056˚ to 0.057˚ and in declination from 0.046˚ to 0.045˚. Estimates of RCS accuracies changed more, suggesting that the sample size in the earlier analysis was too small. Normalized Right Ascension uncertainties decreased from 0.171˚ to 0.151˚ and declination uncertainties decreased from 0.137˚ to 0.102˚. Normalized RA and declination samples were combined in actual operations, yielding a single a priori constraint for both normalized RA and declination. At the end of orbital operations, this constraint was 0.052˚ for ME burns and 0.138˚ for RCS burns. These values are now used for the uniform reconstruction of Cassini's trajectory described in reference [11].

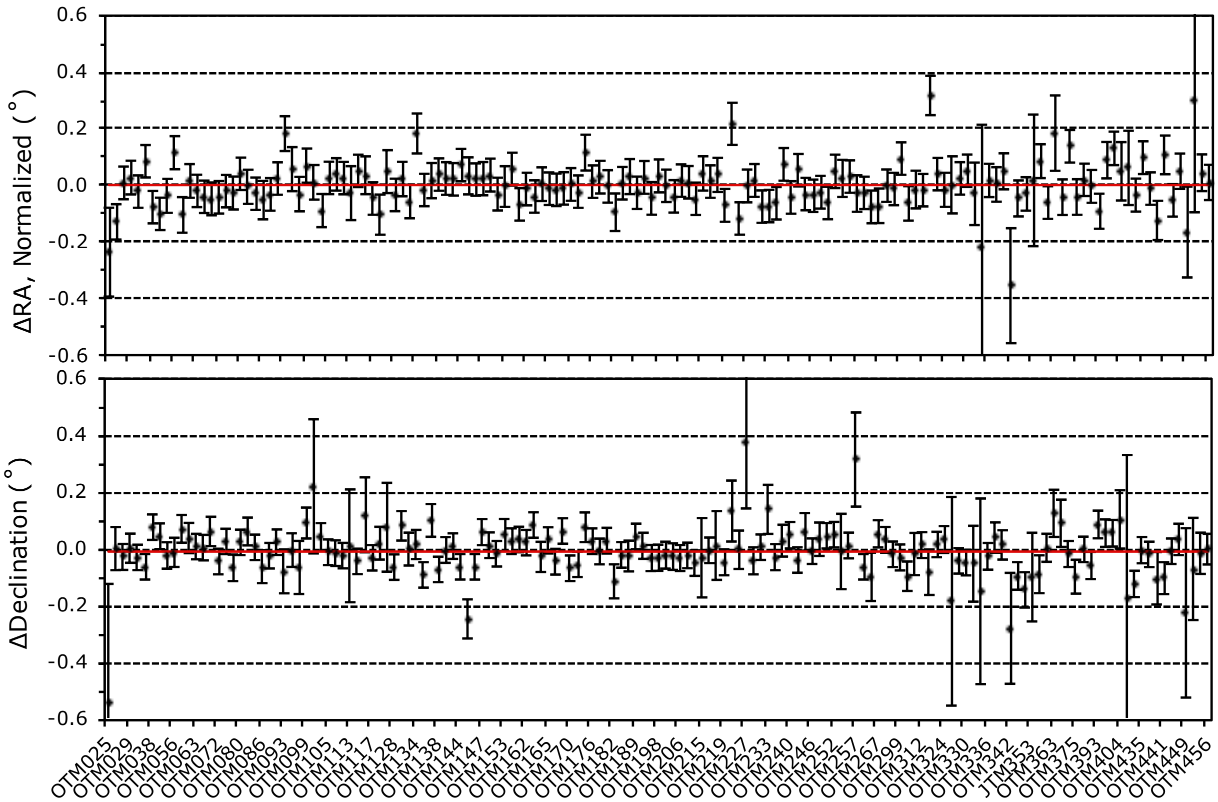

Fig. 3 ME Maneuver ΔV Differences: Navigation Reconstruction Minus Telemetry Computations.

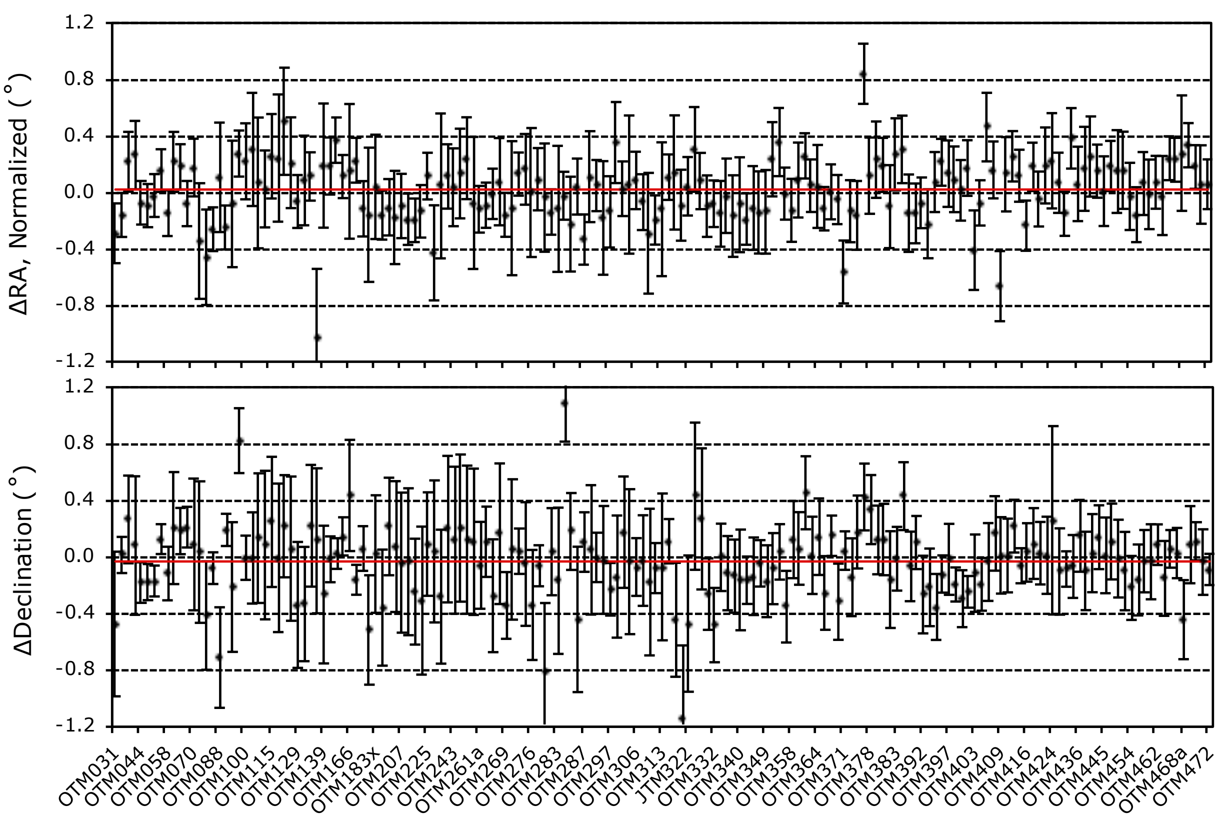

Fig. 4 RCS Maneuver ΔV Differences: Navigation Reconstruction Minus Telemetry Computations.

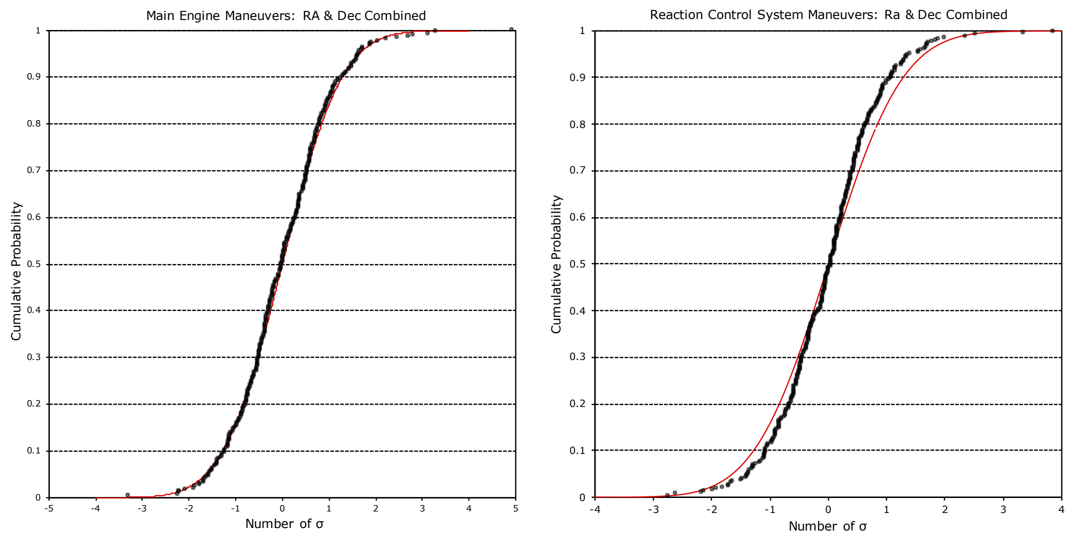

Fig. 5 Cumulative Probability of Main Engine (left) and Reaction Control System (right) Maneuver Errors.

C. Y-Thruster Calibrations

Navigators noticed after executing OTM-169 (the E6/T46 approach maneuver in October 2008) that the burn magnitude was 2.2 sigma lower than anticipated. Upon further investigation, the project determined that two of eight A-branch RCS thrusters were severely degraded and began making preparations to swap to the redundant B-branch. The leading theory for cause of the degradation was related to propellant throughput, and an effort was made to more evenly distribute propellant through the B-branch thrusters. The project also began monitoring the thrusters more closely for future signs of degradation. The four uncoupled Z-facing thrusters were used routinely for RCS maneuvers and a degradation in one of them would become apparent as a change in thruster duty cycle. Monitoring the four coupled Y-facing thrusters would require additional attention. As part of the monitoring, the project adopted an annual calibration test of the Y-thrusters. A sign of degradation in the Y-thrusters would appear as less well coupled thrusters.

Cassini's Z-thrusters were used for RCS maneuvers and attitude control about the spacecraft's X- and Y-axes. The Y-thrusters were used for attitude control about the spacecraft's Z-axis. A diagram of the RCS thruster locations on Cassini and a schematic showing ΔV directions imparted by each thruster are shown in Figure 6.

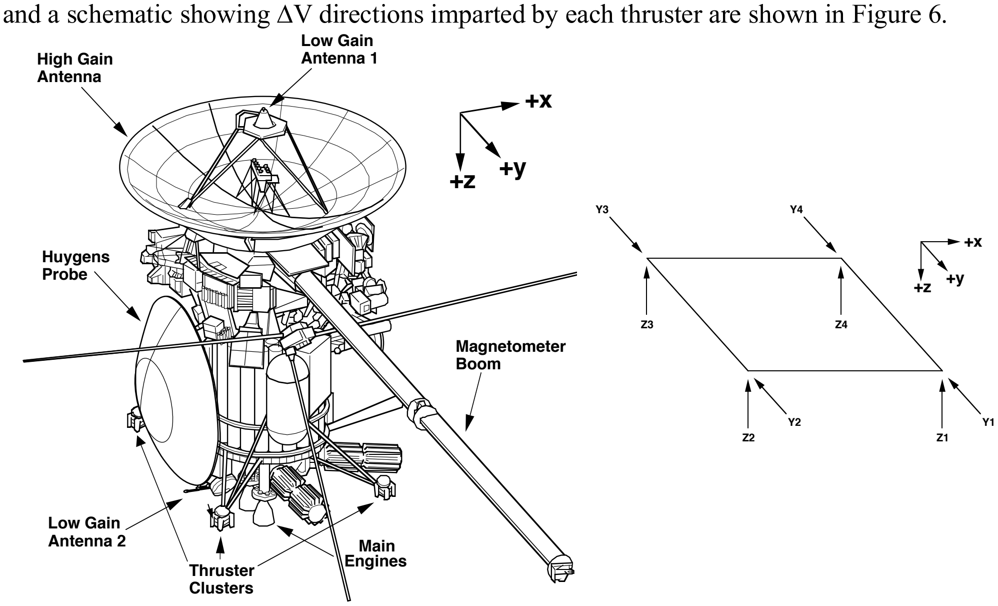

Fig. 6 Cassini Thruster Configuration.

Each Y-thruster calibration began with a quiescent spacecraft—high gain antenna (HGA) pointed at Earth and collecting Doppler tracking data. After at least an hour of coherent Doppler data was acquired, reaction wheels were used to yaw Cassini 90˚ and align its −Y-axis and Y-thrusters toward the Earth-line. Tracking was interrupted because the HGA was no longer pointed toward Earth. Reaction wheels were then spun up in a manner to change angular momentum only along the spacecraft Z-axis, causing one of the Y-thruster couples (Y2 and Y4, or Y1 and Y3) to begin firing. The calibration was designed to spin up reaction wheels as much as possible without ever exceeding operationally safe limits. This produced the most thruster firings and largest ΔV. Ideally, for perfectly coupled thrusters, no ΔV would be imparted to the spacecraft. When complete, the spacecraft yawed −90˚ back to Earth point and at least one more hour of coherent Doppler data was acquired. The spacecraft then repeated this process, but reversed the wheel spin up direction, causing the other Y-thruster couple to fire. When complete and the HGA was returned to Earth point, wheel speeds would be the same as at the calibration start and each set of Y-thruster couple firings was bracketed by coherent Doppler data. This tracking data could then be used to determine the ΔV imparted to Cassini from each couple and hence the mismatch within each couple.

Seven calibrations were performed between the OTM-169 anomaly and Saturn atmospheric entry. One could not be evaluated because a tracking station hardware malfunction prevented acquisition of tracking data. Results from the remaining six are shown in Figure 7. Thruster mismatch remained below 2.5% for each couple in each test, even when accounting for the one-sigma error bars. An initial upward trend in the Y1/Y3 couple caused some concern, but later reversed itself. Ultimately, no degradation was detected in the Y-thrusters.

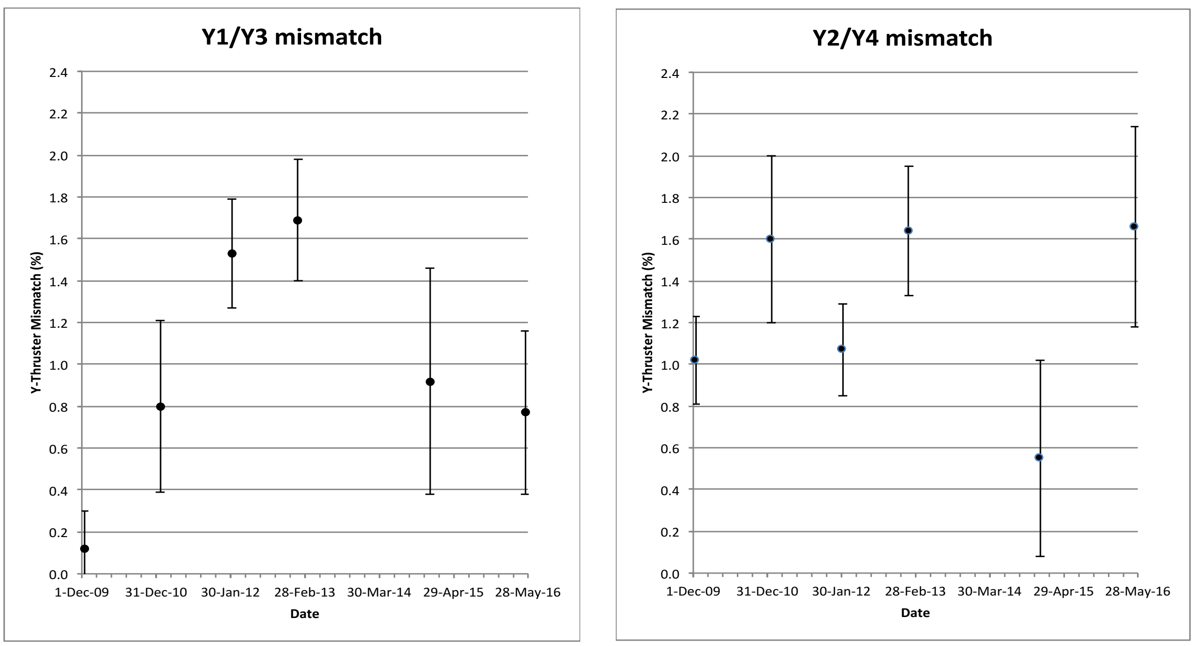

Fig. 7 Thruster Mismatch Determined from Each Y-Thruster Calibration.

IV. Optical Navigation Adaptations

Cassini optical navigation images (opnavs) are pictures of satellites against a background of known stars and were used to determine the spacecraft and satellite positions relative to one another. Prior to collecting and filtering Cassini opnavs, Saturn-centered satellite ephemeris uncertainties were hundreds of kilometers for most of the icy satellites. One-sigma Mimas and Phoebe uncertainties were largest at over one thousand kilometers. Titan ephemeris uncertainties were approximately 150 km. Yet, the first targeted Titan flyby was at an altitude of only 1200 km and because of the satellite's thick atmosphere, safety issues were a concern for altitudes below about 950 km. Clearly, opnavs were needed to fly the Cassini mission and an opnav campaign to reduce satellite ephemeris uncertainties began in February 2004, five months before Saturn orbit insertion.

Initially, Cassini was commanded to image multiple satellites immediately before and after most downlink periods. Images were placed in the 'critical' playback partition in Cassini's Solid State Recorder (SSR) for immediate playback at the start of the next downlink period. During this period of the mission, opnavs made significant improvements in the orbit determination process and the latest images were desired to produce the best ephemeris for use in maneuver designs and onboard ephemeris updates. Opnavs were acquired at the average rate of approximately three images per day through October 2005. From this date through July 2009, nearly halfway through the Equinox extended mission, an average of only four images per week was needed because the satellite ephemeris and Saturnian system parameters (masses, poles, and gravity fields) were markedly improved.

Eventually, ephemeris accuracies obtained through radio-metric sensing of the satellite gravitational signature from multiple satellite close flybys surpassed that from opnavs. Repeated flybys of Titan, the 'engine' of Cassini's tour, kept Titan's ephemeris in check. Titan opnavs, the least accurate because Titan's thick atmosphere prevents its center from being well determined, quickly became unnecessary and were not targeted after April 2006. Close flybys of the other satellites with significant masses (Mimas, Enceladus, Tethys, Dione, Rhea, Hyperion, and Iapetus) were less frequent, however. Opnavs of these satellites continued to be necessary, albeit at a low rate, to prevent runoff in the along-track direction due to errors in mean motion. A small number of high value images was carefully selected to accomplish this goal. From July 2009 until September 20, 2016, the date of Cassini's last opnav, opnavs were acquired at the rate of 1.1 images per month. Each of the images was selected to reveal position errors in the satellite's along-track direction—the minimum angle between the satellite's Saturn relative velocity and Cassini-satellite line-of-sight direction was 60˚ (50˚ for Iapetus). It was not necessary to place any of these opnavs in the SSR's critical playback partition.

V. Maneuver Design Adaptations

A total of 185 maneuvers were planned during Prime Mission, 101 in Equinox Mission, and 214 in Solstice Mission. For each maneuver planned, a prime maneuver was scheduled at the desired time, and a backup maneuver was generally scheduled 24 hours later as a contingency to compensate for being unable to perform the prime maneuver. Typically, three maneuvers were planned within each transfer between targeted flybys: a clean-up maneuver to reduce the growth of downstream errors after a targeted flyby, a shaping maneuver which targets the next flyby, and an approach maneuver to minimize errors at the next flyby. Clean-up and shaping maneuvers were generally 'deterministic', i.e., their reference trajectory ΔV values were non-zero. The approach maneuver was 'statistical', i.e., its reference trajectory ΔV value was always zero and the maneuver would not be needed if orbit determination and maneuver execution errors from the shaping maneuver were insignificant.

Pre-Mission statistical maneuver analyses were conducted to determine mean, one-sigma, and 90% or 95% ΔVs for individual maneuvers and the entire mission assuming each prime maneuver was executed. Maneuvers were often canceled in flight operations however, and sometimes a backup maneuver would be performed instead of a prime maneuver. For these reasons, the statistical analysis for each transfer was updated just prior to entering that transfer based on the latest trajectory information.

During the design of each maneuver in operations, prime, backup, and cancellation opportunities were examined in parallel, with the downstream deterministic cost of each scenario compared. Downstream deterministic costs were determined for maneuvers in three or four additional transfers, by which time the trajectory would normally re-converge to the reference. On rare occasions for backup maneuvers incurring significant ΔV costs, the trajectory might not re-converge in this time frame, but these high-cost backups were analyzed in previous studies to identify mitigation strategies. Maneuver cancellation scenarios resulting in a trajectory that did not re-converge within this time frame were not viable cancellation candidates.

A. Maneuver Execution Errors

Maneuver execution error models are a necessary component when estimating the amount of propellant needed to fly a mission. They also provide *a priori* constraints for the orbit estimation process and a measure for assessing the performance of an executed maneuver. Navigators implemented the Gates model [12] to account for Cassini maneuver errors. The Gates model includes four independent error sources, each assumed to have a Gaussian distribution. These sources are fixed and proportional magnitude errors and fixed and proportional pointing errors. The standard deviation for both magnitude and pointing errors is a function of the maneuver magnitude. Thus, while the model is Gaussian for any given maneuver, it is not Gaussian for a set of maneuvers with different ΔV magnitudes. A maximum likelihood estimator was utilized to determine the four Gates model error sources, with each maneuver equivalent to one sample [13].

Cassini's twenty year operational lifespan made possible several updates to the execution error model for both of Cassini's propulsive systems: the bi-propellant Main Engine Assembly (MEA) used for burns larger than 250 mm/s and the monopropellant Reaction Control System (RCS) used for smaller burns (Fig. 7). Flight software corrections and changes to maneuver design methodology and operational procedures were often implemented to reduce maneuver errors and these changes affected the models.

The first update was introduced after Trajectory Correction Maneuver 13 (TCM-13: cruise maneuvers were designated as TCMs whereas tour maneuvers were called OTMs). Seven large main engine maneuvers were used to estimate and update the proportional MEA error model terms. The new model accounted for several improvements made after these first TCMs to improve future maneuver accuracy [14]. Two flight software corrections, both relating to the accelerometer, were made after TCM-2. An operational procedure was changed after a 0.9˚ pointing bias was detected from the Deep Space Maneuver, TCM-5. The new procedure removed the bias by adding an offset wind turn between completion of the turns to the biased burn attitude and burn start, and a corresponding unwind turn was added after the burn completed. This procedure was implemented from TCM-6 onward. A maneuver design methodology change was implemented beginning with TCM-10. This change reduced fixed magnitude errors by modeling two more ΔVs associated with the maneuver. One of these ΔVs, of magnitude 7.6 mm/s, was due to the newly added offset turns. The other was an unanticipated but consistent ΔV of 3 mm/s, observed when transitioning from a loose to tighter attitude control deadband. Within tour operations, this deadband tightening ΔV would increase to 5 mm/s due to mass property changes after Huygens probe separation and large maneuvers such as SOI and PRM. Similarly, the offset turns ΔV reduced to 6.1 mm/s.

Before mission end, four more updates had been introduced to each of the MEA and RCS models [15]. For the most part, updates were no longer made in response to observations noted from individual burns, procedural changes, or design methodology changes. Instead, the larger number of maneuvers allowed identification of biases in each of the four model terms. Once identified, some biases could be reduced via simple flight software corrections of parameters thought to be causing them, thereby driving the errors toward zero. From the four MEA models, two corrections to the accelerometer scale factor were made to drive down proportional magnitude errors and two corrections to a thruster tail-off parameter were made to drive down fixed magnitude errors. From the four RCS models, two corrections were made to predicted thrust levels to drive down proportional magnitude errors. Pointing error biases were more difficult to reduce and, other than the initial large bias detected from TCM-5, were small enough to be ignored.

One procedural change was implemented in the RCS model as Cassini approached Saturn and attitude control became more commonly performed with reaction wheels rather than thrusters. Turns to the burn attitude were accomplished with reaction wheels, imparting no ΔV to Cassini. This allowed the fixed pointing model error to be zeroed. A fixed magnitude model error remained, primarily because of attitude control deadbanding after completion of the burn. The ΔV imparted was directed along the burn vector and was occasionally updated in the maneuver design process.

The reduction of model errors is apparent in Table 2 and 3, where pre-launch errors may be compared with values used at the end of the mission (2012-1). The final operational main engine model was developed in 2012 from an analysis of 48 main engine maneuvers following a fuel-side tank repressurization in January 2009 (OTMs 180–326). The final operational RCS model was developed from an analysis of 20 RCS maneuvers following a swap to the redundant B-branch thrusters in March 2009 (OTMs 183x–328). A final examination of model parameters was conducted in 2016 [16]. For this analysis, 26 additional main engine maneuvers and 86 additional RCS maneuvers were available. Because changes from 2012-1 were small, neither the MEA model (2016-1L) nor the RCS model (2016-1B) were adopted for use in operations.

Table 2. Main Engine Execution Error Models (1-σ).

		Pre-Launch	2012-1	2016-1L
Magnitude	Proportional (%)	0.35	0.02	0.02
	Fixed (mm/s)	10.0	3.5	3.75
Pointing (per axis)	Proportional (mrad)	10.0	1.0	1.3
	Fixed (mm/s)	17.5	5.0	3.9

Table 3. RCS Execution Error Models (1- σ).

		Pre-Launch	2012-1	2016-1B
Magnitude	Proportional (%)	2.0	0.4	0.3
	Fixed (mm/s)	3.5	0.5	0.6
Pointing (per axis)	Proportional (mrad)	12.0	4.5	4.15
	Fixed (mm/s)	3.5	0	0

B. Target Biasing

The fundamental goal of Cassini navigation was to maintain the spacecraft close to the optimally designed reference trajectory. This reference trajectory defined a sequence of targeted Titan and icy satellite flybys that served as a series of control points. The maneuver strategy targeted the spacecraft to achieve these control points reliably in a manner that minimized ΔV cost and enabled science objectives to be met.

Generally, flyby targets changed only as a result of reference trajectory updates. After nearly three years in orbit, however, the Saturn system was well characterized and orbit determination estimates converged more quickly and accurately. Predicted ΔVs from attitude control activities were improved, thereby improving predictions of Cassini's orbit. Maneuver execution errors were reduced, thereby reducing downstream orbit dispersions. As a result, it occasionally became necessary or advantageous to bias the target.

Target biases were sometimes necessary in order to reduce target errors. As trajectory models improved and maneuver execution errors were reduced, trajectory control improved. Errors remaining after the shaping maneuver were sometimes too small to be corrected with the approach maneuver because the required ΔV was less than the smallest realizable maneuver (15.8 mm/s) allowed by project management. Canceling the maneuver and leaving the target errors uncorrected could have downstream ΔV cost consequences of up to one hundred times larger than the cost of the desired approach maneuver. To avoid large downstream ΔV costs, the two spatial B-plane target components were left unchanged and the time of closest approach was biased from the reference enough to achieve the minimum allowable maneuver magnitude. By doing so, the desired gravity assist ΔV would be obtained at a slightly earlier or later time with little impact to downstream costs.

An example of implementing a time bias is provided by OTM-409, the T111 approach maneuver. The initial maneuver design had a magnitude of 6 mm/s, much smaller than the minimum allowed value of 15.8 mm/s. It would make a correction of 1.2 km in the B-plane and -0.4 seconds in time of closest approach. The downstream cost of canceling this maneuver was found to be approximately 440 mm/s, seventy times larger than the magnitude of the initial design. A simple linearized analysis was performed to prepare Fig. 8 from which was concluded that the bias must be either at least 0.62 seconds earlier or 1.11 seconds later than nominal. Usually, the smaller of the two biases was chosen, but reaction wheel speed considerations sometimes made the larger value more desirable. In this case, the target time was biased 0.7 seconds earlier and the downstream cost was only 40 mm/s, saving 400 mm/s over the cancellation scenario.

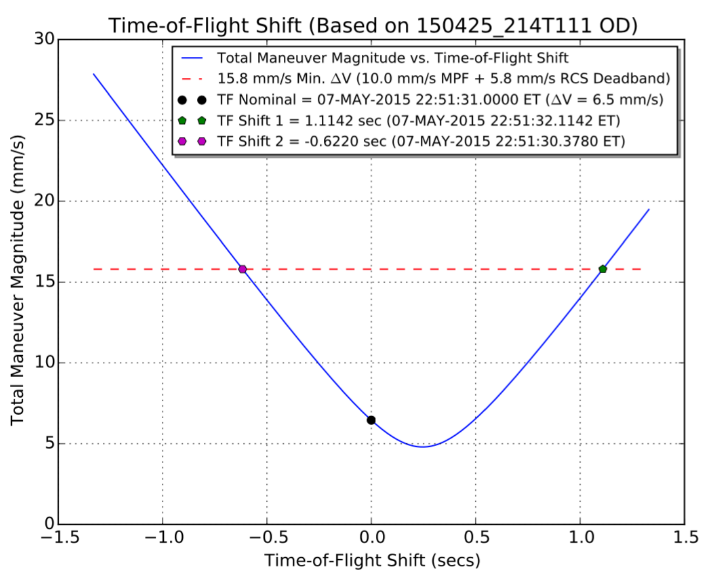

Fig. 8 OTM-409 Target Time Bias vs. ΔV Cost.

Target biases were sometimes advantageous to reduce downstream ΔV costs. The cumulative effect of small modeling errors and canceled maneuvers caused the operational trajectory to deviate from the reference over time. Eventually, the deviations would become large enough that future reference trajectory targets were noticeably nonoptimal, increasing ΔV costs. This effect could be corrected by occasionally introducing a small bias to the target's spatial components, B·R and B·T, leveraging the gravity assist to steer the actual trajectory back toward the reference trajectory.

An example of implementing a B-plane bias is provided by OTM-460, the T123 approach maneuver. The initial maneuver design to the flyby target defined in the reference trajectory was 6.8 mm/s, again too small to perform. In this case, however, a time bias was not necessary. A contour plot (Fig. 9) showing downstream ΔV cost increases as a function of B-plane targets clearly shows that the target from the reference trajectory, the red '+', is not optimal. Choosing the optimal B-plane target instead increased the maneuver size to 24.5 mm/s and decreased the downstream cost by 350 mm/s. In this figure, the blue '+' and ellipse represent the current orbit determination estimate with one-sigma uncertainty. The black '+' and ellipse represents the optimal target and one-sigma delivery uncertainty. The black '+' is not centered within the smallest cost contour because the contour plot is based on a linear analysis. If, during the maneuver design process, the contour plots show an advantage by biasing the B-plane target, a second analysis is undertaken to find the true optimal target.

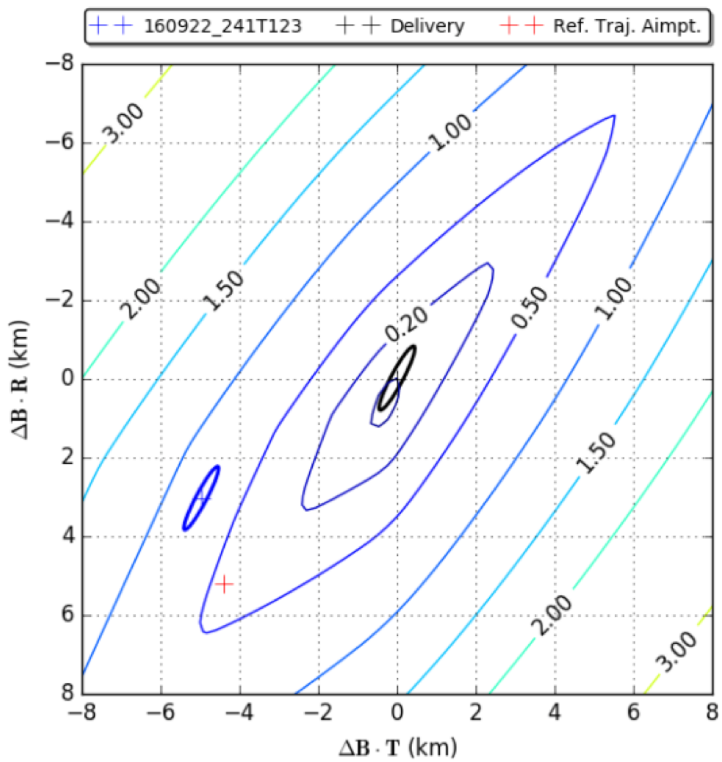

Fig. 9 OTM-460 Downstream ΔV Cost Contours.

Contour plots were originally developed to determine the likelihood of canceling a maneuver [17], which is another way of introducing a target bias. The cost of canceling a maneuver was deduced by determining which contours are crossed by the orbit determination solution. In Fig. 9, the orbit estimate error ellipse runs parallel to the cost contours, so the cost of canceling OTM-460 could be confidently determined as 700 mm/s. The shape, size, and orientation of orbit determination error ellipses as a function of data cutoff were determined by covariance analyses before the start of a particular transfer. Superimposing the ellipse from the final data cutoff onto the target point provides an early estimate of the range of expected downstream costs if the maneuver were to be performed.

In total, 15 flybys were targeted with time biases. The first time-biased target was implemented with OTM-106 at the T29 flyby. The first of 14 B-plane biases was implemented at the following flyby, T30, with OTM-109 [18]. Before project approval of any target bias, a preliminary trajectory including the bias was provided to science planners. Planners would use it to evaluate the effect of the bias on their observations. Usually, these biases were small enough to have no significant effect on the observations. On rare occasions when a bias did impact observations, however, three options were considered and discussed: remove the bias and pay the resulting ΔV cost, keep the bias and degrade the science, or keep the bias and update the sequence to maintain the full integrity of the observation. Of course, the third option was always preferred if possible after considering workforce and time constraints.

C. Backup Maneuver Scheduling

Statistical analyses were not generally conducted for backup maneuvers because of the large number of possible permutations and because ΔV costs for backup maneuvers scheduled 24 after the prime were generally expected to remain viable. Navigators discovered two scenarios however, that caused backup maneuver costs to grow considerably larger than if the prime maneuver were implemented.

The first backup maneuver scenario leading to large ΔV growth was identified during early operational designs of OTM-159. This maneuver had a large deterministic cost of 12 m/s and would execute less than two hours before periapsis. The backup opportunity, only nine hours after the prime, cost 33 m/s, almost three times more than the prime. Additionally, downstream ΔV costs required to remain near the reference trajectory increased dramatically, such that the total cost became 97 m/s and was prohibitively large. To reduce the risk of needing to perform the backup OTM-159, ground controllers sent maneuver commands to Cassini three days before the planned maneuver execution and confirmed that they were received and registered onboard the spacecraft. Normally, maneuver commands were sent only six hours before maneuver execution so that orbit determination errors were minimized. If a ground antenna was experiencing difficulties and was unable to send commands, commanding would be delayed until the beginning of the next track and the backup maneuver would be implemented. Had the prime OTM-159 maneuver opportunity been missed, navigators had developed backup scenarios that reduced the total cost from 97 m/s to as little as 8 m/s. However, these scenarios significantly altered as many as six of the next seven Titan flybys and removed E6, a 200 km Enceladus flyby, altogether. Science return would be degraded and diminished, and a significant command sequence update effort would be needed to recover the best science observations.

Shortly after the OTM-159 prime maneuver was successfully executed, navigators examined the remaining set of currently existing maneuvers to identify any similar future instances of a large deterministic maneuver near periapsis. Four were found in Equinox Mission: OTMs 168, 170, 180, and 183. Two years later, with a reference trajectory for Solstice Mission available, three more were identified: OTMs 261, 300, and 312. An analysis of the backup maneuver for each of these maneuvers was conducted. In every case except OTM-168, maneuver commands were sent to the spacecraft early to ensure that the prime maneuver would be executed. Backup maneuver scenarios were investigated and, as with OTM-159, each required significant changes to downstream targets before the backup opportunity became viable. The backup scenario for OTM-168 was not as extreme as the other scenarios, with downstream costs growing to only 4.3 m/s. There were only three tracks between OTM-168 and the preceding OTM-167, so sending maneuver commands early risked basing the maneuver design on a poorly converged orbit estimate. Instead, an additional tracking station was placed on standby, ready to send prime maneuver commands if there were a transmitter problem with the primary station. Also, backup maneuver commanding, if necessary, would be performed at a different Deep Space Network complex to mitigate the very unlikely risk that an entire complex was down for the prime maneuver and could not be brought back up in time to send backup maneuver commands.

The second backup maneuver scenario leading to large ΔV growth was identified during early operational designs of OTM-268. In this case, the backup maneuver was nearly singular with central angle travel to the E12 target of 179.3°. Because of the near singularity, ΔV gradients for each of the target parameters became nearly aligned, causing a large ΔV to be needed in one direction to make a small correction in one of the target parameters. Whereas the cost of prime maneuver was only 65 mm/s and could be accurately performed via the RCS thrusters, the backup maneuver grew nearly an order of magnitude to 580 mm/s and, unless mitigated, would be executed less accurately on the MEA. Making matters worse, the target was a low 50 km altitude flyby of Enceladus. An accurate flyby was especially important because of the high visibility associated with it. To mitigate the backup maneuver cost, one of three targeted parameters, B·R, was allowed to 'float', or miss the target by a controlled amount. By allowing B·R to miss the target by −0.5 km, the backup maneuver cost was reduced from 580 mm/s to only 115 mm/s and the −0.5 km float was insignificant compared to the one-sigma 2.7 km orbit determination uncertainty.

Navigators were confident that future 'n-pi' transfers could be dealt with similarly. The experience gained from OTM-268 would allow them to quickly recognize future incidents in flight operations. For these reasons and because backup maneuvers were rarely needed, a pre-emptive examination of all maneuvers to identify and flag future n-pi transfers was deemed unnecessary.

VI. Software Adaptations

As with any other operational project, navigators developed numerous scripts to assist with the more mundane tasks of planning, estimating, and controlling Cassini's trajectory. Two software sets were especially notable however, for their breadth and impact on navigation operations: the Maneuver Automation Software (MAS), and the Mission Analysis, Operations, and Navigation Toolkit Environment (MONTE). A third software tool, MONTE-MOPS, generated a report for each maneuver design. This report was notable for providing information from which key navigation decisions were made.

MAS was developed during cruise operations for use in tour to address the need for a faster maneuver design and implementation process. With only 24 maneuvers scheduled in the nearly seven years of interplanetary cruise, a speedy process was not of critical importance. The typical process starting from the availability of the final orbit determination solution and ending with the availability of ready-for-uplink maneuver commands typically lasted five days. During tour operations, this changed. A typical Titan-to-Titan transfer would require three maneuvers in sixteen days and the final orbit determination solution required sufficient time to re-converge the orbit after the perturbation from the previous maneuver. The clean-up maneuver would be the most demanding. To keep ΔV costs low, the maneuver was typically scheduled three days after the targeted flyby, and the first two days after were needed to re-converge the orbit estimate. This could leave less than 24 hours for design, implementation, and uplink of the maneuver.

MAS shortened this process from five days to as little as five hours. Files not dependent on the final orbit estimate were prepared in advance. Each subsystem was responsible for configuring their portion of the software within MAS but, once configured, interfaces between each subsystem were automated. MAS would perform all of the necessary checks and provide a report at the end of the process with the result of each check. This report would be reviewed and, as appropriate, approved by all teams before uplink to the spacecraft. Once properly configured, intermediate MAS runs could easily be performed as the day-to-day orbit determination solution changed. These intermediate runs were important for addressing failed checks or other problems and ensured that the final run would successfully complete with a set of commands to execute the desired maneuver.

Python and C++ based MONTE software replaced the Jet Propulsion Laboratory's legacy software set—the Fortran based Double Precision Trajectory/Orbit Determination Program (DPRTAJ/ODP) and Maneuver Operations Software (MOPS). Due to declining support for the legacy software and to ensure Cassini navigators would have the needed skills to work on other missions, the navigation team began using MONTE operationally at the end of 2011. The transition was preceded with an extensive two year development, test, and checkout period in which MONTE was run in parallel with legacy software, ensuring all needed capabilities were available and functioning correctly.

As the mission progressed, maneuver presentations for project reviews evolved to encompass designs for the prime, backup, cancellation, and alternate maneuvers. MONTE-MOPS was augmented to automatically assemble a comprehensive presentation package consisting of the prime and backup design history, comparisons of ΔV costs, and trajectory deviation plots. This report generation tool was essential for providing information needed for making informed decisions regarding various maneuver options.

VII. Conclusion

Navigation of the Cassini spacecraft during over a decade of orbital operations at Saturn required the flight team to adapt to new or changed requirements and to take advantage of improvements in knowledge, procedures, and the computing environment. The navigation team performed splendidly, meeting all their requirements and enabling two successful extended missions. Knowledge gained of Saturn and its satellites may be used by future projects, and the techniques developed by Cassini navigators will be used by other projects as well.

Appendix

Table 4. Cassini Prime Mission Reference Trajectory Targeted Encounters.

Encounter	Satellite	Time (UTC)	In / Out	Altitude [km]	B-Plane [deg]	V-Infinity [km/s]	Period [days]	Inc. [deg]	Rev
Ta	Titan	26-Oct-04 15:30	I	1200	-39	5.65	47.9	13.8	a
Tb	Titan	13-Dec-04 11:38	I	1200	-59	5.64	31.9	5.4	b
Tc	Titan	14-Jan-05 11:12	I	60000	180	5.37	31.8	5.3	c
T3	Titan	15-Feb-05 06:58	I	1577	-30	5.58	20.4	0.4	3
E1	Enceladus	09-Mar-05 09:08	I	500	150	6.60	20.5	0.2	4
T4	Titan	31-Mar-05 20:05	O	2402	-147	5.61	16.0	7.4	5
T5	Titan	16-Apr-05 19:12	O	1025	-76	5.63	18.2	21.6	6
E2	Enceladus	14-Jul-05 19:55	I	175	145	8.17	18.3	21.8	11
T6	Titan	22-Aug-05 08:54	O	3669	120	5.61	16.0	15.6	13
T7	Titan	07-Sep-05 08:12	O	1075	67	5.65	18.4	0.3	14
H1	Hyperion	26-Sep-05 02:25	O	510	124	5.64	18.2	0.3	15
D1	Dione	11-Oct-05 17:52	I	500	120	9.10	17.9	0.4	16
T8	Titan	28-Oct-05 04:15	I	1353	181	5.54	27.4	0.4	17
R1	Rhea	26-Nov-05 22:38	I	500	10	7.29	27.4	0.4	18
T9	Titan	26-Dec-05 19:00	O	10409	180	5.49	23.4	0.4	19
T10	Titan	15-Jan-06 11:41	I	2043	180	5.48	39.2	0.4	20
T11	Titan	27-Feb-06 08:25	O	1813	180	5.51	23.3	0.4	21
T12	Titan	19-Mar-06 00:06	I	1951	180	5.47	39.2	0.4	22
T13	Titan	30-Apr-06 20:58	O	1855	180	5.49	23.3	0.4	23
T14	Titan	20-May-06 12:18	I	1879	180	5.48	39.2	0.4	24
T15	Titan	02-Jul-06 09:21	O	1906	180	5.48	23.3	0.4	25
T16	Titan	22-Jul-06 00:25	I	950	-92	5.52	24.0	14.9	26
T17	Titan	07-Sep-06 20:17	I	1000	-24	5.54	16.0	24.5	28
T18	Titan	23-Sep-06 18:59	I	960	-81	5.52	15.9	37.6	29
T19	Titan	09-Oct-06 17:30	I	980	-75	5.53	15.9	46.6	30
T20	Titan	25-Oct-06 15:58	I	1030	-10	5.54	12.0	54.9	31
T21	Titan	12-Dec-06 11:41	I	1000	-123	5.51	15.9	52.8	35
T22	Titan	28-Dec-06 10:05	I	1300	-61	5.53	15.9	56.5	36
T23	Titan	13-Jan-07 08:39	I	1000	-52	5.53	15.9	59.2	37
T24	Titan	29-Jan-07 07:16	I	2631	-69	5.53	18.1	58.8	38
T25	Titan	22-Feb-07 03:12	O	1000	-56	5.82	15.9	58.6	39
T26	Titan	10-Mar-07 01:49	O	980	-48	5.82	15.9	56.0	40
T27	Titan	26-Mar-07 00:23	O	1010	-58	5.82	15.9	52.3	41
T28	Titan	10-Apr-07 22:58	O	990	-66	5.82	15.9	46.8	42
T29	Titan	26-Apr-07 21:33	O	980	-73	5.81	15.9	39.1	43
T30	Titan	12-May-07 20:10	O	960	-79	5.81	15.9	28.2	44
T31	Titan	28-May-07 18:52	O	2300	-84	5.81	16.0	18.0	45
T32	Titan	13-Jun-07 17:46	O	975	-87	5.81	16.0	2.1	46
T33	Titan	29-Jun-07 17:00	O	1932	-9	5.84	22.8	0.4	47
T34	Titan	19-Jul-07 01:11	I	1332	-179	5.85	39.7	0.3	48
T35	Titan	31-Aug-07 06:33	O	3326	-117	5.82	32.0	6.1	49
I1	Iapetus	10-Sep-07 14:16	O	1644	176	2.34	32.0	6.1	49
T36	Titan	02-Oct-07 04:43	O	975	120	5.88	23.8	5.0	50
T37	Titan	19-Nov-07 00:47	O	1000	158	5.88	16.0	12.0	52
T38	Titan	05-Dec-07 00:07	O	1300	96	5.90	16.0	26.0	53
T39	Titan	20-Dec-07 22:58	O	970	101	5.91	15.9	37.7	54
T40	Titan	05-Jan-08 21:30	O	1010	166	5.90	12.0	46.6	55
T41	Titan	22-Feb-08 17:32	O	1000	140	5.92	10.6	56.1	59
E3	Enceladus	12-Mar-08 19:06	I	56	90	14.41	10.6	56.1	61
T42	Titan	25-Mar-08 14:28	O	1000	147	5.93	9.6	63.1	62
T43	Titan	12-May-08 10:02	O	1000	-161	5.92	8.0	69.3	67
T44	Titan	28-May-08 08:25	O	1400	-170	5.91	7.1	74.7	69
T45	Titan	31-Jul-08 02:13	O	1613	127	5.88	7.4	74.5	78
E4	Enceladus	11-Aug-08 21:06	I	54	90	17.73	7.4	74.5	80

In/Out = flyby inbound (I) or outbound (O). B-plane = B-plane angle relative to the satellite's pole (H1 angle is relative to Saturn pole). Period = spacecraft period after encounter. Inc. = inclination after encounter wrt Saturn's equator. Rev = project rev # of flyby.

Table 5. Cassini Equinox Mission Reference Trajectory Targeted Encounters.

Encounter	Satellite	Time (UTC)	In / Out	Altitude [km]	B-Plane [deg]	V-Infinity [km/s]	Period [days]	Inc. [deg]	Rev
E5	Enceladus	09-Oct-08 19:07	I	28	90	17.7	7.3	74.5	88
E6*	Enceladus	31-Oct-08 17:15	I	200	90	17.7	7.3	74.5	91
T46	Titan	03-Nov-08 17:35	O	1100	7	5.87	7.9	70.6	91
T47	Titan	19-Nov-08 15:56	O	1023	151	5.86	8.0	72.3	93
T48	Titan	05-Dec-08 14:26	O	960	164	5.86	8.0	73.1	95
T49	Titan	21-Dec-08 13:00	O	970	110	5.86	9.4	74.7	97
T50	Titan	07-Feb-09 08:51	O	960	60	5.87	11.9	65.3	103
T51	Titan	27-Mar-09 04:44	O	960	114	5.86	16.8	63.3	106
T52	Titan	04-Apr-09 01:48	I	4150	179	5.53	16.0	61.7	107
T53	Titan	20-Apr-09 00:21	I	3600	169	5.54	16.0	61.3	108
T54	Titan	05-May-09 22:54	I	3244	158	5.54	15.9	60.6	109
T55	Titan	21-May-09 21:27	I	965	147	5.55	16.0	58.7	110
T56	Titan	06-Jun-09 20:00	I	965	133	5.55	16.0	55.7	111
T57	Titan	22-Jun-09 18:33	I	955	122	5.55	15.9	51.2	112
T58	Titan	08-Jul-09 17:04	I	965	113	5.54	15.9	44.5	113
T59	Titan	24-Jul-09 15:34	I	955	106	5.54	15.9	34.7	114
T60	Titan	09-Aug-09 14:04	I	970	100	5.54	16.0	20.8	115
T61	Titan	25-Aug-09 12:52	I	970	161	5.53	24.0	12.1	116
T62	Titan	12-Oct-09 08:36	I	1300	61	5.56	19.0	0.5	118
E7	Enceladus	02-Nov-09 07:42	O	100	90	7.74	19.0	0.5	119
E8	Enceladus	21-Nov-09 02:10	I	1604	82	7.75	19.0	0.5	120
T63	Titan	12-Dec-09 01:03	O	4850	-147	5.47	16.0	4.9	122
T64	Titan	28-Dec-09 00:17	O	955	-95	5.49	16.0	21.6	123
T65	Titan	12-Jan-10 23:11	O	1073	86	5.50	16.0	5.2	124
T66	Titan	28-Jan-10 22:29	O	7490	53	5.53	17.5	0.3	125
R2	Rhea	02-Mar-10 17:41	I	100	-99	8.55	17.6	0.4	127
T67*	Titan	05-Apr-10 15:51	I	7462	180	5.51	20.8	0.4	129
D2	Dione	07-Apr-10 05:16	I	504	0	8.36	20.4	0.3	129
E9	Enceladus	28-Apr-10 00:10	O	100	90	6.51	20.5	0.3	130
E10*	Enceladus	18-May-10 06:05	I	439	147	6.52	20.5	0.3	131
T68	Titan	20-May-10 03:24	O	1400	131	5.48	16.0	12.1	131
T69	Titan	05-Jun-10 02:26	O	2044	-89	5.49	16.0	2.0	132
T70	Titan	21-Jun-10 01:28	O	880	-93	5.49	16.0	19.1	133
T71	Titan	07-Jul-10 00:23	O	1005	56	5.50	19.9	4.5	134
E11	Enceladus	13-Aug-10 22:31	I	2552	90	6.84	20.0	4.6	136
T72	Titan	24-Sep-10 18:39	O	8175	15	5.53	23.8	3.0	138

In/Out = flyby inbound (I) or outbound (O). B-plane = B-plane angle relative to the satellite's pole (H1 angle is relative to Saturn pole). Period = spacecraft period after encounter. Inc. = inclination after encounter wrt Saturn's equator. Rev = project rev # of flyby. * = Encounter is not targeted but has targeted encounter characteristics.

Table 6. Cassini Solstice Mission Reference Trajectory Targeted Encounters.

Encounter	Satellite	Time (UTC)	In / Out	Altitude [km]	B-Plane [deg]	V-Infinity [km/s]	Period [days]	Inc. [deg]	Rev
T73	Titan	11-Nov-10 13:37	O	7921	144	5.44	20.6	0.0	140
E12	Enceladus	30-Nov-10 11:54	O	50	-119	6.26	20.6	0.1	141
E13	Enceladus	21-Dec-10 01:08	O	50	-61	6.22	20.7	0.1	142
R3	Rhea	11-Jan-11 04:53	O	75	103	8.02	20.4	0.3	143
T74	Titan	18-Feb-11 16:04	I	3651	180	5.49	27.9	0.4	145
T75	Titan	19-Apr-11 05:01	O	10053	180	5.42	23.4	0.4	147
T76	Titan	08-May-11 22:54	I	1873	180	5.51	39.1	0.4	148
T77	Titan	20-Jun-11 18:32	O	1359	180	5.49	21.7	0.4	149
T78	Titan	12-Sep-11 02:50	I	5821	0	5.61	17.7	0.3	153
E14	Enceladus	01-Oct-11 13:52	I	100	90	7.43	17.8	0.2	154
E15	Enceladus	19-Oct-11 09:22	I	1236	14	7.48	17.8	0.2	155
E16	Enceladus	06-Nov-11 04:59	I	500	151	7.38	17.9	0.2	156
D3*	Dione	12-Dec-11 09:39	O	100	-175	8.70	17.5	0.2	158
T79	Titan	13-Dec-11 20:11	O	3586	-8	5.49	23.5	0.9	158
T80	Titan	02-Jan-12 15:14	I	29415	120	5.44	24.2	1.6	159
T81	Titan	30-Jan-12 13:40	O	31131	120	5.39	23.5	1.4	160
T82	Titan	19-Feb-12 08:43	I	3803	-10	5.55	17.9	0.4	161
E17	Enceladus	27-Mar-12 18:30	I	75	87	7.48	17.8	0.4	163
E18	Enceladus	14-Apr-12 14:02	I	75	93	7.48	17.8	0.4	164
E19	Enceladus	02-May-12 09:31	I	75	108	7.51	17.8	0.4	165
T83	Titan	22-May-12 01:10	O	955	-107	5.43	16.0	15.8	166
T84	Titan	07-Jun-12 00:07	O	959	-40	5.45	23.9	21.1	167
T85	Titan	24-Jul-12 20:03	O	1012	-111	5.43	21.2	32.2	169
T86	Titan	26-Sep-12 14:36	O	956	-91	5.44	23.9	39.0	172
T87	Titan	13-Nov-12 10:22	O	973	-163	5.42	15.9	46.3	174
T88	Titan	29-Nov-12 08:57	O	1014	-144	5.42	13.3	53.0	175
T89	Titan	17-Feb-13 01:57	O	1978	-149	5.42	12.0	57.1	181
R4	Rhea	09-Mar-13 18:17	I	1000	-132	9.27	12.0	57.0	183
T90	Titan	05-Apr-13 21:44	O	1400	161	5.42	9.6	61.7	185
T91	Titan	23-May-13 17:33	O	970	-90	5.44	12.0	59.4	190
T92	Titan	10-Jul-13 13:22	O	964	-93	5.44	16.0	56.7	194
T93	Titan	26-Jul-13 11:56	O	1400	-82	5.44	23.9	53.4	195
T94	Titan	12-Sep-13 07:44	O	1400	-119	5.43	31.9	51.9	197
T95	Titan	14-Oct-13 04:56	O	961	-134	5.43	47.9	49.7	198
T96	Titan	01-Dec-13 00:41	I	1400	132	5.44	31.9	51.3	199
T97	Titan	01-Jan-14 22:00	I	1400	148	5.43	31.9	50.1	200
T98	Titan	02-Feb-14 19:13	I	1236	131	5.43	31.9	48.1	201
T99	Titan	06-Mar-14 16:27	I	1500	119	5.43	31.9	45.5	202
T100	Titan	07-Apr-14 13:41	I	963	121	5.43	35.8	40.7	203
T101	Titan	17-May-14 16:12	O	2994	120	5.36	31.9	44.3	204
T102	Titan	18-Jun-14 13:28	O	3659	111	5.36	31.9	46.5	205
T103	Titan	20-Jul-14 10:41	O	5103	115	5.36	31.9	48.0	206
T104	Titan	21-Aug-14 08:09	O	964	-65	5.39	31.9	44.6	207
T105	Titan	22-Sep-14 05:23	O	1400	-72	5.39	31.9	40.3	208
T106	Titan	24-Oct-14 02:41	O	1013	-47	5.39	47.8	33.1	209
T107	Titan	10-Dec-14 22:27	O	980	-114	5.38	31.9	28.6	210
T108	Titan	11-Jan-15 19:49	O	970	-84	5.38	31.9	19.1	211
T109	Titan	12-Feb-15 17:08	O	1200	-87	5.38	31.9	8.5	212
T110	Titan	16-Mar-15 14:30	O	2275	-105	5.38	28.0	0.3	213
T111	Titan	07-May-15 22:50	I	2721	1	5.38	18.9	0.3	215
D4	Dione	16-Jun-15 20:12	O	517	-80	7.31	18.9	0.4	217
T112	Titan	07-Jul-15 08:10	O	10953	-1	5.47	21.8	0.5	218
D5	Dione	17-Aug-15 18:33	I	479	-96	6.43	21.9	0.4	220
T113	Titan	28-Sep-15 21:37	I	1036	1	5.40	13.9	0.6	222
E20	Enceladus	14-Oct-15 10:41	I	1846	-78	8.51	13.9	0.6	223
E21	Enceladus	28-Oct-15 15:23	O	50	96	8.49	13.9	0.6	224
T114	Titan	13-Nov-15 05:47	O	11920	166	5.35	12.7	1.3	225
E22	Enceladus	19-Dec-15 17:49	O	5000	-178	4.22	12.9	1.3	228
T115	Titan	16-Jan-16 02:20	O	3548	19	5.45	15.9	4.1	230
T116	Titan	01-Feb 16 01:00	O	1400	94	5.42	16.0	17.5	231
T117	Titan	16-Feb-16 23:50	O	1018	41	5.43	23.9	21.9	232
T118	Titan	04-Apr-16 19:43	O	990	72	5.42	31.9	28.8	234
T119	Titan	06-May-16 16:55	O	971	100	5.41	31.9	36.0	235
T120	Titan	07-Jun-16 14:06	O	975	131	5.40	23.9	43.0	236
T121	Titan	25-Jul-16 09:58	O	976	168	5.40	16.0	49.2	238
T122	Titan	10-Aug-16 08:31	O	1698	-167	5.40	12.0	53.7	239
T123	Titan	27-Sep-16 04:17	O	1774	-153	5.40	9.6	57.9	243
T124	Titan	13-Nov-16 23:56	O	1584	-135	5.40	8.0	61.4	248
T125	Titan	29-Nov-16 22:15	O	3158	-131	5.39	7.2	63.7	250
T126	Titan	22-Apr-17 06:08	O	979	-103	5.40	6.4	62.4	270

In/Out = flyby inbound (I) or outbound (O). B-plane = B-plane angle relative to the satellite's pole (H1 angle is relative to Saturn pole). Period = spacecraft period after encounter. Inc. = inclination after encounter wrt Saturn's equator. Rev = project rev # of flyby. * = Encounter is not targeted but has targeted encounter characteristics.

Acknowledgments

The research described in this publication was carried out at the Jet Propulsion Laboratory, California Institute of Technology, under a contract with the National Aeronautics and Space Administration. Copyright 2018 California Institute of Technology. Government sponsorship acknowledged.

References

[1] N. J. Strange, B. B. Buffington and J. B. Jones, "In-Flight Modification of the Cassini Reference Trajectory," AIAA/AAS Astrodynamics Specialist Conference and Exhibit, AIAA Paper 2008-6750, Honolulu, HI, August 18 - 21, 2008. doi: 10.2514/6.2008-6750.

[2] B. Buffington, N. Strange and R. Ionasescu, "Addition of a Low Altitude Tethys Flyby to the Nominal Cassini Tour," AAS/AIAA Astrodynamics Specialist Conference, AAS 05-270, Lake Tahoe, CA, August 7 - 11, 2005.

[3] F. J. Pelletier, B. B. Buffington, N. Strange and T. Denk, "Re-Aiming Cassini's Iapetus Flyby," AAS/AIAA Astrodynamics Specialist Conference, AAS 07-255, Mackinac Island, MI, August 19 - 23, 2007.

[4] "Huygens Recovery Task Force Final Report," ESA Report HUY-RP-12241, July 27, 2001.

[5] J. Bordi, P. Antreasian, J. Jones, C. Meek, R. Ionasescu, I. Roundhill and D. Roth, "Orbit Determination Results and Trajectory Reconstruction for the Cassini/Huygens Mission," Jet Propulsion Laboratory, National Aeronautics and Space Administration, Pasadena, CA, 2005.

[6] N. J. Strange, T. D. Goodson and Y. Hahn, "Cassini Tour Redesign for the Huygens Mission," AIAA/AAS Astrodynamics Specialist Conference and Exhibit, AIAA 2002-4720, Monterey, CA, August 5 - 8, 2002.

[7] C. J. Hansen, L. W. Esposito, K. -M. Aye, J. E. Colwell, A. R. Hendrix, G. Portyankina and D. Shemansky, "Investigation of diurnal variability of water vapor in Enceladus' plume by the Cassini ultraviolet imaging spectrograph," AGU Publications, Geophysical Research Letters, 2017. doi: 10.1002/2016GL071853.

[8] P. Antreasian, J. Bordi, K. Criddle, R. Ionasescu, R. Jacobson, J. Jones, R. MacKenzie, M. Meek, F. Pelletier, D. Roth, I. Roundhill and J. Stauch, "Cassini Orbit Determination Performance During the First Eight Orbits of the Saturn Satellite Tour," AAS/AIAA Astrodynamics Specialists Conference, AAS 05-312, Lake Tahoe, CA, August 7 - 11, 2005.

[9] D. L. Matson, J. C. Castillo-Rogez, G. Schubert, C. Sotin and W. B. McKinnon, "The Thermal Evolution and Internal Structure of Saturn's Mid-Sized Icy Satellites," in *Saturn From Cassini-Huygens*, Dordrecht, Springer, 2009, pp. 577-612.

[10] D. C. Roth, P. G. Antreasian, S. M. Ardalan, K. E. Criddle, T. Goodson, R. Ionasescu, J. B. Jones, D. W. Parcher, F. J. Pelletier, P. F. Thompson and A. T. Vaughan, "Navigational Use of Cassini ΔV Telemetry," AIAA/AAS Astrodynamics Specialist Conference and Exhibit, AIAA 2008-6746, Honolulu, HI, August 18 - 21, 2008. doi: 10.2514/6.2008-6746.

[11] J. Bellerose, D. Roth, K. Criddle, D. Boone, R. Ionasescu and Z. Tarzi, "The Cassini Mission: Reconstructing Thirteen Years of the Most Complex Gravity-Assist Trajectory Flown to Date," SpaceOps 2018 Conference, Marseille, France, 2018.

[12] C. R. Gates, "A Simplified Model of Midcourse Maneuver Execution Errors," JPL, Technical Report 32-504, Pasadena, CA, October 15, 1963.

[13] S. V. Wagner and T. D. Goodson, "Execution-Error Modeling and Analysis of the Cassini-Huygens Spacecraft Through 2007," AAS/AIAA Space Flight Mechanics Meeting, AAS 08-113, Galveston, TX, January 27-31, 2008.

[14] T. D. Goodson, D. L. Gray, Y. Hahn and F. Peralta, "Cassini Maneuver Experience: Finishing Inner Cruise," AAS/AIAA Space Flight Mechanics Meeting, AAS 00-167, Clearwater, FL, January 23-26, 2000.

[15] S. V. Wagner, "Maneuver Performance Assessment of the Cassini Spacecraft Through Execution-Error Modeling and Analysis," AAS/AIAA Space Flight Mechanics Meeting, AAS 14-390, Santa Fe, NM, January 26-30, 2014.

[16] S. V. Wagner, "Cassini Maneuver Performance Assessment and Execution-Error Modeling Through 2015," AAS/AIAA Space Flight Mechanics Meeting, AAS 16-305, Napa, CA, February 14-18, 2016.

[17] P. Stumpf, E. Gist, T. Goodson, Y. Hahn, S. Wagner and P. Williams, "Flyby Error Analysis Based on Contour Plots for the Cassini Tour," *Journal of Spacecraft and Rockets,* vol. 46, no. 5, pp. 1016-1022. doi: 10.2514/1.42143, September-October 2009.

[18] P. N. Williams, E. Gist, T. Goodson, Y. Hahn, P. Stumpf and S. Wagner, "Cassini-Huygens Maneuver Experience: Third Year of Saturn Tour," AAS/AIAA Astrodynamics Specialist Conference, AAS 07-254, Mackinac Island, MI, August 19-23, 2007.